Investigation of transient wave behavior in water pipelines with blockages

X. F. Yan[1]; **H. F. Duan**, *M.ASCE*[2]; **X. K. Wang**[3]; **M. L. Wang**[4]; **P. J. Lee**[5]

[1] Assistant Professor, State Key Laboratory of Hydraulics and Mountain River Engineering, Sichuan University, Chengdu, 610065, China. (*Former Research Associate in the Department of Civil and Environmental Engineering at The Hong Kong Polytechnic University, Hong Kong SAR, 999077, China*). E-mail: xufeng.yan@scu.edu.cn.

[2] Associate Professor, Department of Civil and Environmental Engineering, The Hong Kong Polytechnic University, Hung Hom, Kowloon, Hong Kong SAR 999077, China. (*Corresponding Author*), E-mail: hf.duan@polyu.edu.hk.

[3] Professor, State Key Laboratory of Hydraulics and Mountain River Engineering, Sichuan University, Chengdu, 610065, China. E-mail: wangxiekang@scu.edu.cn.

[4] Research Assistant (PhD Student), Department of Civil and Environmental Engineering, The Hong Kong Polytechnic University, Hung Hom, Kowloon, Hong Kong SAR 999077, China. E-mail: manli.wang@polyu.edu.hk.

[5] Professor, Department of Civil and Natural Resources Engineering, University of Canterbury, Private Bag 4800, Christchurch, New Zealand. Email: pedro.lee@canterbury.ac.nz.

Abstract: Partial blockages commonly exist in water pipelines due to various physical, chemical and biological processes, including sediment, corrosion and biofilm. The formed blockages can result in low flowing capacity, additional energy loss and water quality deterioration during water conveyance process such as urban water supply and drainage systems. This paper presents an investigation on the interaction of transient pressure waves with pipe-wall roughness and blockages in water pipelines. The analytical expression of wave propagation in a pipeline with rough blockages is firstly derived by the multi-scale wave perturbation analysis for transient pipe flows. The analytical results and analysis demonstrate that the wave scattering (amplitude damping and phase shifting) is dependent on the relationship between the incident wavelength and the correlation length of roughness-blockage disorders in the pipeline. The relative importance of pipe-wall roughness friction and pipe blockage constriction to the wave scattering in terms of wave envelope attenuation and wave phase change is then investigated based on the analytically derived results. Two dimensionless parameters, which are functions of the properties of incident waves, pipe-wall roughness, blockage severity and range, and internal fluid conditions, are formulated to characterize such relevance and importance. For validation, the analytical results are compared with experimental data collected in this study based on a laboratory experimental test system designed for the former study. Finally, the key results and findings of this study are discussed for their applicability and implication to transient pipe flow modelling and pipeline condition assessment in practical applications.

Keywords: Water pipeline; Transient flow; Roughness; Blockage; Wave scattering;

Introduction

Waterhammer, which is also termed as fast transients, hydraulic transients or pressure surges in the literature, commonly exists in fluid piping system with its theory development and practice dated back to 1900s (Ghidaoui et al., 2005). Modelling and simulation of waterhammer phenomena is important to both the transient pipe system design (Wylie et al., 1993; Duan et al., 2010a; Chaudhry, 2014) and the pipeline condition assessment (Brunone, 1999; Duan et al., 2011a, 2012; Lee et al., 2013; Meniconi et al., 2013; Gong et al., 2014, 2016, 2018; Duan and Lee, 2016; Kim, 2016, 2020; Wang and Ghidaoui, 2018; Che et al., 2018, 2019; Ayati et al., 2019; Wang et al., 2019; Keramat et al., 2020; Zouari et al., 2019, 2020). To accurately represent and reproduce waterhammer results in a practical pipeline system, various factors have been considered and coupled into the waterhammer/transients models, such as the formulas and expressions for pipe-skin friction and fluid turbulence (Vardy and Brown, 1995; Brunone and Berni, 2010;), pipe-wall material visco-elasticity (Covas et al., 2005; Duan et al., 2010b; Meniconi et al., 2012; Guidara et al., 2018; Pan et al., 2020, 2021), fluid column separation (Bergant et al., 2006; Ramezani and Karney, 2017), fluid-structure interaction (Wiggert and Tijsseling, 2001; Bergant et al., 2006; Keramat et al., 2012; Zanganeh et al., 2020; Zouari et al., 2019), and air-fluid interaction (Wright et al., 2011; Zhou et al., 2013; Zhu et al., 2018). With the understanding and model development of physical mechanisms and process of transient pipe flows, substantial progress and improvements have been made for the waterhammer theory and practice (Wylie et al., 1993; Chaudhry, 2014; Ghidaoui et al., 2005). However, significant discrepancies between the model predictions and data measurements can still be commonly found in many practical applications under different conditions and such differences become especially significant in aged pipeline systems (McInnis and Karney, 1995; Ebacher et al., 2011;

66 Meniconi et al., 2015).

67 In addition to the accuracy improvement of physical models and numerical schemes
68 (Ghidaoui et al., 2005), uncertainty and complexity can usually play important roles in affecting
69 the applicability of such models in practical applications. For this inspection, some recent studies
70 have attributed part of this profound difference to the wave scattering effect (i.e., wave amplitude
71 damping and phase shifting). In complex pipe systems, wave scattering may be induced by the
72 variations and irregularities of cross-sectional areas along pipelines (which is termed as rough
73 blockages in this study), which usually cannot be represented by the roughness-induced friction
74 only in these pipeline systems (Duan, 2017; Duan et al., 2017). An analytical expression has
75 been derived in that study for the wave behaviors in pipelines with rough blockage induced by
76 the irregular variations of pipe diameters. The multi-scale analysis method, which was widely
77 used in other fields of hydrodynamics such as shallow water waves (Lu, 2008), water pipelines
78 (Duan et al., 2014; Duan, 2017) and artery blood hammer (Mei and Jing, 2016), has been
79 successfully applied to transient pipe flow systems. The results gained in that study demonstrated
80 the important influence of wave scattering on the transient envelope attenuation (amplitude
81 damping) and phase change (frequency shifting).

82 In practice, it is important to study the transient interactions of pressure waves and internal
83 pipe conditions for understanding transient wave propagation process, thereby its utilization for
84 pipeline diagnosis (e.g., Duan et al., 2011a, 2014, 2017; Meniconi et al., 2011, 2015; Kim 2016;
85 Wang et al., 2019; Zouari et al., 2019, 2020), especially in the complex and aged pipeline
86 systems, where the random and irregular variations of pipe diameters become more and more
87 severe due to many unavoidable factors (Stephens, 2008; Ebacher et al., 2011) such as corrosion,
88 bio-film, deposition, and complex connections of pipes and/or facilities with different sizes

89 shown in Fig. 1. For instance, the inspection of an aged water supply pipeline that was still in use
90 revealed that over 50% of pipe cross-sectional area was blocked along that pipe section
91 (Stephens, 2008; Duan et al., 2017; Gong et al., 2018). Such blockages may have significant
92 hydraulic effect on the mainstream flow motions (and thus transient waves) along the pipeline,
93 which is different from the traditional pipe-wall friction effect that induces energy dissipation
94 only within the boundary layer. Consequently, an in-depth understanding of the interaction of
95 transient waves and pipe-wall conditions (roughness and blockages) will be crucial to transient
96 modelling and utilization for water supply system analysis.
97
98 Fig. 1 will be here.
99
100 In the previous studies (Duan, 2017; Duan et al., 2017), the assumptions of frictionless
101 pipelines and inviscid pipe flows have been made for analytical derivations, in order to highlight
102 and separate the effect of wave scattering from others such as friction and turbulence. Thereafter,
103 numerical and experimental applications by different researchers have shown the consistent
104 results with the previously derived analytical results in terms of the importance of wave
105 scattering in transient pipe flow systems (Wu and Fricke, 1990; Duan et al., 2011b; Lee et al.,
106 2015; Meniconi et al., 2015; Duan et al., 2017). Numerical simulations in these studies have also
107 demonstrated that the wave behaviors in such disordered pipelines cannot be represented by the
108 friction and turbulence models only. On the basis of these previous studies, it is necessary to
109 further understand and analyze the physical mechanism of wave scattering effect induced by the
110 pipe-wall disorders and its importance and relevance to pipe roughness-blockage factors, which
111 is the scope of this study.

This paper aims to examine the relative importance and influence of wave scattering resulted from pipe roughness and blockage factors to the transient wave behaviors. The multi-scale analytical method is adopted in this study to obtain a comprehensive perspective of wave scattering analysis in the transient pipe flow system with rough blockages along the pipeline. As continuous and preliminary study, two situations of transient laminar and small-amplitude turbulent flows are considered in this paper, because they have become increasingly important to the transient-based pipe diagnosis and condition analysis (Brunone, 1999; Duan et al., 2011a; Lee et al., 2013; Gong et al., 2014; Meniconi et al., 2015; Kim, 2016; Ayati et al., 2019; Zanganeh et al., 2020). The obtained results are then used to analyze and discuss the influence and relevance of wave-roughness-blockage interaction to the transient modelling and analysis at the end of this paper. Finally, the analytical results are validated by the experimental data collected in this study from the laboratory experimental pipeline system that was designed for the former study (Duan et al., 2017).

Models and Method of Investigation

The wave equation used for analytical analysis in this study is firstly described based on the classic transient flow models by considering the pipe-wall friction effect. Meanwhile, the multi-scale wave perturbation method that is used for the analytical derivation is presented in this section for clarification.

Transient flow model

The one-dimensional (1D) transient wave model for slightly compressible and unsteady flows in pipes is adopted in this study for the investigation, and the continuity and momentum equations

can be expressed as follows (Ghidaoui et al., 2005; Chaudhry, 2014):

$$\frac{\partial Q}{\partial x}+\frac{A}{\rho a^2}\frac{\partial P}{\partial t}=0, \tag{1}$$

$$\frac{\partial Q}{\partial t}+\frac{A}{\rho}\frac{\partial P}{\partial x}+\frac{\pi D}{\rho}\tau_w=0, \tag{2}$$

where Q = flowrate; A = pipe cross-sectional area; a = wave speed; D = pipe diameter; ρ = fluid density; P = pressure; x, t = spatial and temporal coordinates; and τ_w = wall shear stress, and can usually be expressed by the Darcy–Weisbach formula as,

$$\tau_w=\frac{\rho f|Q|}{8A^2}Q, \tag{3}$$

in which f = the Darcy friction factor. Considering that transient perturbations are given by $Q = Q_0+q$ and $P = P_0+p$, with Q_0, P_0 = initial steady-state flowrate and pressure, and q, p = transient parts of flowrate and pressure, the governing equations (1) and (2) becomes:

$$\frac{\partial q}{\partial x}+\frac{A}{\rho a^2}\frac{\partial p}{\partial t}=0, \tag{4}$$

$$\frac{\partial q}{\partial t}+\frac{A}{\rho}\frac{\partial p}{\partial x}+\frac{\pi D}{\rho}\tau_w^p=0, \tag{5}$$

where $\tau_w = \tau_{w0} + \tau_w^p$, with τ_{w0}, τ_w^p being average (steady) and perturbing (transient) components of wall shear stress. Particularly:

(1) For laminar flow regime: $f=\frac{64}{\mathbf{Re}_0}$ with $\mathbf{Re}_0=\frac{Q_0 D}{A_0\nu}$ is initial Reynolds number and ν is kinematic viscosity. Under this condition, Eq. (5) becomes,

$$\frac{\partial q}{\partial t}+\frac{A}{\rho}\frac{\partial p}{\partial x}+\frac{8\pi\nu}{A}q=0. \tag{6}$$

(2) For turbulent flow regime: f is a function of pipe size, pipe-wall roughness, and flow

condition ($\mathbf{Re}_0$), which can be usually determined by the empirical Colebrook–White equation (Wylie et al., 1993; Ghidaoui et al., 2005; Chaudhry, 2014). Assuming small-amplitude transient flows with $Q = Q_0 >> q$, Eq. (2) can be simplified as,

$$\frac{\partial q}{\partial t} + \frac{A}{\rho}\frac{\partial p}{\partial x} + \frac{f|Q|}{DA}q = 0 . \tag{7}$$

Combining Eq. (4) and Eq. (6) or Eq. (7), by eliminating one of the variables (e.g., q here), gives a general form of the wave equation for describing both transient laminar flows and small-amplitude transient turbulent flows as,

$$A\left(\frac{\partial^2 p}{\partial t^2}\right) - a^2 \frac{\partial}{\partial x}\left(A\frac{\partial p}{\partial x}\right) = \pm Ka\frac{\partial p}{\partial x} , \tag{8}$$

where K is friction coefficient, with $K = 8\pi\nu$ for transient laminar flow case, and $K = 0.25\pi\nu f\mathbf{Re}_0$ for small-magnitude transient turbulent flows; the signs "±" denote the directions of base flow (towards upstream and downstream respectively) as indicated in Eq. (3). In this study, "–" is taken in Eq. (8) for example in the following analytical derivations (i.e., base flow is from upstream to downstream), and the similar analysis for the "+" case (i.e., base flow from downstream to upstream) can be obtained by the same derivation procedure. Meanwhile, the small-amplitude transient turbulent flow case is considered in this study since it has been very important to the transient-based applications for pipe condition assessment such as leakage and blockage detection (Meniconi et al., 2011; Lee et al., 2013; Gong et al., 2014, 2018; Wang et al., 2019; Zouari et al., 2020).

It is also worthy of noting that: (i) the convective inertia term in the momentum Eq. (2) has been neglected due to the very small March number ($\mathbf{M}=a/V << 1$) for water hammer flows (Ghidaoui et al., 2005; Mei and Jing, 2016); (ii) the linearization of turbulent friction in Eq. (7) is valid for the small-amplitude transient flows, which has been evidenced in the previous study

175 (Duan et al., 2018); and (iii) the source term on the right-hand side of Eq. (8) is the main
176 difference from the frictionless pipeline case investigated in previous studies (Duan et al., 2011b;
177 Duan, 2017; Gong et al., 2018; ; Zouari et al., 2019), but the form of Eq. (8) has a great
178 difference from the cases for other fields of hydrodynamics such as shallow water wave and pure
179 acoustic waves where the method of multi-scale analysis has also been applied to perform the
180 analytical analysis (Wu and Fricke, 1990; Colton et al., 2000; Lu, 2008).
181
182 ***Multi-scale wave analysis***
183 Multi-scale analysis has been widely developed and applied in solving wave perturbation and
184 scattering problems (Colton et al., 2000), such as shallow water waves (Lu, 2008), acoustic
185 waves (Wu and Fricke, 1990), and pipe transient waves (Duan, 2017; Duan et al., 2017). The
186 principle and procedure of multi-scale analysis is to (1) introduce different scale variables (fast-
187 slow and/or large-small) for an independent variable in the original system; (2) treat these multi-
188 scale variables independently to eliminate the secular terms in the system equations; and (3)
189 solve equations for all scale variables (usually one by one) under solvability conditions. For the
190 wave equation (8) of transient pipe flows focused in this study, it has,
191 (i) independent variables:
192 $$x = x; x_1 = \varepsilon x; x_2 = \varepsilon^2 x...; \text{ and } t = t; t_1 = \varepsilon t; t_2 = \varepsilon^2 t...; \quad (9)$$
193 (ii) dependent variable:
194 $$p = p_0(x, x_1, x_2, t, t_1, t_2) + \varepsilon p_1(x, x_1, x_2, t, t_1, t_2) + \varepsilon^2 p_2(x, x_1, x_2, t, t_1, t_2) + ..., \quad (10)$$
195 where ε is scaling variable, and subscripts "0, 1, 2…" represent the order of multiple scales. As a
196 result, it has,

197 $$\frac{\partial}{\partial x}=\frac{\partial}{\partial x}+\varepsilon\frac{\partial}{\partial x_1}+\varepsilon^2\frac{\partial}{\partial x_2}+\ldots;\ \text{and}\ \frac{\partial}{\partial t}=\frac{\partial}{\partial t}+\varepsilon\frac{\partial}{\partial t_1}+\varepsilon^2\frac{\partial}{\partial t_2}+\ldots\ . \quad (11)$$

198 In pipe fluid transients, multi-scale wave analysis becomes relevant and significant for both
199 physical understanding and practical applications. Specifically, transient wave propagation in the
200 pipeline system is affected by many factors, such as pipe skin friction and turbulence, junctions,
201 pipe faults, pipe material deformation, and system boundaries. The influences of these factors
202 result in different wave behaviors, that is, multiple reflections and transmissions in different
203 scales of time and space, so that the responses of the transient system will consist of waves in
204 different scales of space and time. In this study, only the pipe-wall roughness and internal
205 blockages along the pipeline are considered for analysis, which therefore induces three scales of
206 wave propagation in the pipeline. In detail, the transient waves in single pipelines (described by
207 the governing equation (8)) can be divided into following three scales: main wave streams
208 (incident wave) with an order of $\varepsilon^0 = 1$, the reflected waves by pipe blockages with an order of ε,
209 and the smoothed waves by pipe-wall roughness with an order of ε^2. As a result, the first three
210 terms of the right-hand side of the above Eqs. (10) and (11) are included with a truncation of
211 $O(\varepsilon^2)$ for high-order terms (i.e., order > 2) in the following derivations.
212
213 **Analytical Derivation and Results Analysis**
214 The analytical derivation is performed by the multi-scale wave perturbation method. In this
215 section, the main assumptions applied for the derivations are firstly provided, followed by the
216 key results and analysis for wave scattering effect in pipelines.
217
218 ***Important assumptions for analytical derivation***

The important assumptions made in this study for the analytical derivations mainly include:

(1) All the results gained in this study are based on Eq. (8), which is valid for the transient laminar flows (i.e., $\mathbf{Re}_0 < 2000$) and small-amplitude transient turbulent flows (i.e., $q << Q_0$) (Lee et al., 2013; Duan et al., 2018);

(2) The convective inertia in the momentum Eq. (2) has been neglected due to the very small *Mach* number ($\mathbf{M} = a/V << 0$, with $a \sim 1000$ m/s and $V \sim 1$ m/s) for water hammer waves in pressurized water pipelines such as metallic and concrete materials (Ghidaoui et al., 2005);

(3) The variation of pipe cross-sectional area due to rough blockages along the pipeline, as shown in Fig. 2, is represented by the following function (Duan, 2017; Duan et al., 2011b; 2017):

$$A(x) = A_0(1 + \varepsilon\zeta(x)), \tag{12}$$

in which: $\zeta(x)$ characterizes the irregular variation of pipe cross-sectional area, which has zero mean; A_0 is the pipe cross-sectional area for uniform pipeline;

(4) Relatively small transient perturbations from incident waves and pipe area disorders (blockage) compared to original steady (pre-transient) state, and therefore, $|\zeta(x)| << 1$ in Eq. (12).

Fig. 2 will be here

Key results of analytical derivation

Based on the above-mentioned assumptions, applying multi-scale analysis method of Eq. (9) through Eq. (11) to the transient wave equation (8) and neglecting high-order terms (i.e., order >

242 2) provides the derivative results of pressure wave perturbation as follows,

243 $$\frac{\partial p}{\partial x}=\frac{\partial p_0}{\partial x}+\varepsilon\left(\frac{\partial p_1}{\partial x}+\frac{\partial p_0}{\partial x_1}\right)+\varepsilon^2\left(\frac{\partial p_2}{\partial x}+\frac{\partial p_1}{\partial x_1}+\frac{\partial p_0}{\partial x_2}\right), \tag{13}$$

244 $$\frac{\partial^2 p}{\partial t^2}=\frac{\partial^2 p_0}{\partial t^2}+\varepsilon\left(\frac{\partial^2 p_1}{\partial t^2}+2\frac{\partial^2 p_0}{\partial t\partial t_1}\right)+\varepsilon^2\left(\frac{\partial^2 p_2}{\partial t^2}+\frac{\partial^2 p_0}{\partial t_1{}^2}+2\frac{\partial^2 p_1}{\partial t\partial t_1}+2\frac{\partial^2 p_0}{\partial t\partial t_2}\right). \tag{14}$$

245 Then substituting Eq. (12) through Eq. (14) into Eq. (8), and again neglecting the high-order
246 terms, the final results in different scales are obtained as follows:

247 Zero-order (ε^0):

248 $$\frac{\partial^2 p_0}{\partial t^2}-a^2\frac{\partial^2 p_0}{\partial x^2}+\frac{Ka}{A_0}\frac{\partial p_0}{\partial x}=0; \tag{15}$$

249 First-order (ε^1):

250 $$\begin{aligned}&\left(\frac{\partial^2 p_1}{\partial t^2}+2\frac{\partial^2 p_0}{\partial t\partial t_1}+\zeta(x)\frac{\partial^2 p_0}{\partial t^2}\right)\\&=a^2\left(\frac{\partial^2 p_1}{\partial x^2}+2\frac{\partial^2 p_0}{\partial x\partial x_1}+\frac{\partial\zeta(x)}{\partial x}\frac{\partial p_0}{\partial x}+\zeta(x)\frac{\partial^2 p_0}{\partial x^2}\right)-\frac{Ka}{A_0}\left(\frac{\partial p_1}{\partial x}+\frac{\partial p_0}{\partial x_1}\right)\end{aligned}; \tag{16}$$

251 Second-order (ε^2):

252 $$\begin{aligned}&\left(\frac{\partial^2 p_2}{\partial t^2}+\frac{\partial^2 p_0}{\partial t_1{}^2}+2\frac{\partial^2 p_1}{\partial t\partial t_1}+2\frac{\partial^2 p_0}{\partial t\partial t_2}+\zeta(x)\left(\frac{\partial^2 p_1}{\partial t^2}+2\frac{\partial^2 p_0}{\partial t\partial t_1}\right)\right)\\&=a^2\left(\begin{array}{l}\dfrac{\partial^2 p_2}{\partial x^2}+\dfrac{\partial^2 p_0}{\partial x_1{}^2}+2\dfrac{\partial^2 p_1}{\partial x\partial x_1}+2\dfrac{\partial^2 p_0}{\partial x\partial x_2}\\+\dfrac{\partial\zeta(x)}{\partial x}\left(\dfrac{\partial p_1}{\partial x}+\dfrac{\partial p_0}{\partial x_1}\right)+\zeta(x)\left(\dfrac{\partial^2 p_1}{\partial x^2}+2\dfrac{\partial^2 p_0}{\partial x\partial x_1}\right)\end{array}\right)-\frac{Ka}{A_0}\left(\frac{\partial p_2}{\partial x}+\frac{\partial p_1}{\partial x_1}+\frac{\partial p_0}{\partial x_2}\right)\end{aligned}. \tag{17}$$

253 To solve different scale equations above, it is practical and feasible to start the solution
254 process from the zero-order Eq. (15), with assuming its solution form,

255 $$p_0=We^{ikx-i\omega t}, \tag{18}$$

256 where W = wave amplitude; k and ω = wave number and frequency. Combining Eq. (13) and Eq.

(18) gives,

$$\omega = \pm K_\omega a k\,, \tag{19}$$

with $K_\omega = \sqrt{1 + i\frac{K}{A_0 a k}}$ indicating the friction effects (K) to the mainstream wave propagation.

Thereafter, the solution of first-order Eq. (16) can be obtained by considering Eq. (18) and Eq. (19) and applying the Green's function theorem (Lu, 2008), as,

$$p_1 = -\frac{kW}{2\beta} e^{-i\omega t} \int_{-\infty}^{+\infty} e^{\alpha(x-\xi)} e^{i\beta|x-\xi|} e^{ik\xi} \left(\frac{\partial \zeta(\xi)}{\partial \xi} + \frac{K}{A_0 a} \zeta(\xi) \right) d\xi\,. \tag{20}$$

Based on the zero- and first-order solutions, the solvability of the second-order Eq. (17) is obtained for the expression of wave amplitude evolution as follows,

$$\left(\begin{array}{l} \frac{\left(1+K_\omega^2\right)a^2 k}{2\omega}\frac{\partial W}{\partial x_2} + \frac{\partial W}{\partial t_2} \\ -a^2\frac{k^2 W}{4\omega\beta}\left[\int_{-\infty}^{x} \left(C_{x'\xi'} + \frac{K}{A_0 a} C_{x'\xi} \right) d\xi + \left(1 - 2\frac{\beta}{k}\right) \int_{x}^{+\infty} e^{-i2\beta\delta} \left(C_{x'\xi'} + \frac{K}{A_0 a} C_{x'\xi} \right) d\xi \right] \\ -\frac{ik^3 W}{4\omega\beta}\left[\int_{-\infty}^{x} \left(C_{x\xi'} + \frac{K}{A_0 a} C_{x\xi} \right) d\xi + \left(1 - 2\frac{\beta}{k}\right)^2 \int_{x}^{+\infty} e^{-i2\beta\delta} \left(C_{x\xi'} + \frac{K}{A_0 a} C_{x\xi} \right) d\xi \right] \\ +\frac{ikW\omega}{4\beta}\left[\int_{-\infty}^{x} \left(C_{x\xi'} + \frac{K}{A_0 a} C_{x\xi} \right) d\xi + \int_{x}^{+\infty} e^{-i2\beta\delta} \left(C_{x\xi'} + \frac{K}{A_0 a} C_{x\xi} \right) d\xi \right] \end{array} \right) = 0\,. \tag{21}$$

with the coefficient symbols defined by,

$$C_{x\xi} = \sigma^2 \gamma(\delta),\ C_{x\xi'} = \sigma^2 \frac{d\gamma(\delta)}{d\delta},\ C_{xx'} = \sigma^2 \frac{d\gamma(\delta)}{d\delta}(0),\ C_{x'x'} = -\sigma^2 \frac{d^2\gamma(\delta)}{d\delta^2}\,. \tag{22}$$

where $\sigma^2 = \sigma^2(x,\xi)$ = ensemble averaged magnitude of pipe area disorders relative to the mean value as given in Eq. (12); $\gamma(\delta)$ = the correlation coefficient and it is assumed that $\gamma(\delta) = e^{-\theta|\delta|}$ in this study, with θ being spatial correlation factor of pipe disorders and $\delta = x - \xi$ being spatial distance. Consequently, combining Eq. (18) through Eq. (22), the solution of Eq. (21) has the

following form,

$$W = W_0 e^{-\psi X} e^{i\phi Y} \quad , \tag{23}$$

and,

$$\psi = \frac{k\theta\sigma^2}{\theta^2 + 4k^2} + \alpha; \ \phi = \frac{k\theta\sigma^2}{2\theta^2 + 8k^2} - \frac{\alpha^2 k}{2\theta} , \tag{24}$$

where ψ and ϕ are dimensionless factors representing for wave envelope attenuation and wave phase change respectively; X = characteristic distance for wave propagation relative to incident wave length (k); Y = characteristic phase for wave propagation relative to pipe disorder correlation length (θ); $\alpha = K/2A_0\omega$ is friction-related dimensionless damping factor; and other symbols refer to previous definitions in this paper.

Results Analysis

Based on the derived result of Eq. (24), it is necessary to compare the individual contributions of wave scattering by pipe blockage and wave smoothing by pipe-wall roughness to transient wave modifications (amplitude attenuation and phase change). Particularly, two following special cases can be derived (with subscripts "*ws*" and "*fr*" indicating wave scattering by blockage and wave smoothing by roughness, respectively):

(1) For the case of frictionless pipeline or inviscid flow, i.e., $K = 0$ and $\alpha = 0$, it provides the result of wave modification by wave scattering effect of pipe blockages only, as

$$\psi_{ws} = \frac{k\theta\sigma^2}{\theta^2 + 4k^2}; \ \phi_{ws} = \frac{k\theta\sigma^2}{2\theta^2 + 8k^2} . \tag{25}$$

This result indicates clearly the wave scattering effect attains to a maximum as $\theta/k = 2$, which is consistent with the previous result in Duan et al. (2011b, 2017).

(2) Regarding the case of the uniform pipeline without disorders, i.e., $\sigma^2 \to 0$ and $\theta \to +\infty$, it gives the result of wave modification by the friction effect of pipe-wall roughness only, as

$$\psi_{fr} = \alpha;\ \phi_{fr} = -\frac{\alpha^2 k}{2\theta}\ . \tag{26}$$

Therefore, with the existence of wave scattering effects by both pipe blockage and roughness, their relative importance can be described approximately by the following dimensionless parameters for the wave amplitude attenuation and phase change respectively,

$$G_{amp} = \left|\frac{\psi_{fr}}{\psi_{ws}}\right| = \frac{\alpha}{\sigma^2}\frac{\theta^2 + 4k^2}{\theta k};\ G_{pha} = \left|\frac{\phi_{fr}}{\phi_{ws}}\right| = \frac{\alpha^2}{\sigma^2}\frac{k}{\theta}\frac{\theta^2 + 4k^2}{\theta k}. \tag{27}$$

The above analytical results indicate the different modification results and mechanisms of wave scattering effects on the transient wave propagation in the pipeline. Specifically, it is shown that the wave scattering by blockage reflections is highly related to the properties of the pipe disorders and incident waves (σ^2, θ and k), while that by pipe-wall roughness relies mainly on the properties of the fluid and pipe-wall conditions (α). As a result, it can be easily concluded that the relative importance of these two effects depends on the conditions of internal fluid, pipe-wall material and incident waves, with its quantification expressed in Eq. (27). In fact, this result is useful to quantify and examine numerically the influence ranges of these two different effects to transient wave propagation and behaviors, with the perspective to understand their relevance to the transient modelling and analysis under different conditions in practice.

For instance, considering a typical pipeline for urban water supply and drainage systems, the dimensionless parameter α in Eq. (24) and Eq. (27) can be further rewritten as,

$$\alpha = \frac{K}{2A_0\omega} \sim \frac{\nu}{2D_0^2}\frac{L}{a} f\mathbf{Re}_0 \sim \frac{T_w}{T_d} f\mathbf{Re}_0\,, \tag{28}$$

where T_w is longitudinal wave propagation time scale; T_d is radial wave diffusion time scale. Actually, this dimensionless parameter in Eq. (28) has been derived in the previous study (Duan et al., 2012a) to represent the relevance and importance of friction effect in pipe fluid transients. To quantify the different influences of pipe-wall roughness and pipe blockages on wave scattering, following typical orders of the values and ranges for the parameters are adopted for a numerical analysis based on previous studies (Ghidaoui et al., 2005; Duan et al., 2012a),

(1) $T_w \sim 1$; $T_d \sim 10^5$; $f\mathbf{Re}_0 \sim [64, 10^3]$ for rough pipeline flows; so that $\alpha \sim [6.4\times10^{-4}, 10^{-2}]$;

(2) $\sigma^2 \sim 0.1$ for pipe disorders of cross-sectional area; $\theta/k \sim [10^{-2}, 10^{-2}]$ for typical transient pressure waves in water pipelines.

As a result, the influences of pipe-wall friction and rough blockage to transient wave envelope attenuation and wave phase change can be evaluated and plotted in Figs. 3 and 4 respectively, with sub-figures (a) and (b) in each figure for presenting the variation trends of dimensionless parameters (ψ or ϕ) and relative importance coefficients (G_{amp} or G_{pha}) derived formerly in this study.

Fig. 3 will be here.

Fig. 4 will be here.

The results in Figs. 3 and 4 demonstrate the dependence of the relative importance and influence of these two factors (roughness and blockage) to the wave amplitude attenuation and phase change on the disorder-wave ratio θ/k and initial friction condition $f\mathbf{Re}_0$. On first hand, Figs. 3(a) and 4(a) show that the friction effect of pipe-wall roughness could cause additional attenuation percentage of the envelope amplitude for different friction conditions in addition to

337 wave scattering effect of pipe blockages (irregular diameters). However, the pipe-wall friction
338 presents little impact on the wave phase change (frequency shift), which is different from wave
339 scattering effect. Particularly, the condition of maximum wave scattering effect is $\theta=2k$ for all
340 the frictional cases, which is also consistent with the previous result for frictionless pipeline case
341 in Duan (2017) and Duan et al. (2017).

342 On the other hand, Figs. 3(b) and 4(b) indicate that the relative importance of these two
343 factors (i.e., roughness to blockage) to wave behaviors also varies with the two dimensionless
344 parameters of disorder-wave ratio θ/k and friction conditions $f\mathbf{Re}_0$ from the derivations in this
345 study. The overall inspection of these results demonstrates the dominant effect of wave scattering
346 by rough blockages for most cases within the studied domain. Specifically, with regard to wave
347 amplitude attenuation, the pipe-wall friction effect is more important ($G_{amp} > 1$ for the black-
348 filled region in Figs. 3b and 4b) only for the cases of very highly turbulent flows (e.g., $f\mathbf{Re}_0 > 10^2$)
349 and relatively large difference between incident wave length and pipe disorder correlation length
350 (e.g., $\theta/k > 10$ or $\theta/k < 10$), which is consistent with observations in many previous studies (Lee
351 et al., 2015; Duan et al., 2017).

352 Consequently, it can be concluded from Figs. 3 and 4 that the relative importance and
353 influence of pipe-wall roughness to pipe blockage on the transient wave behaviors become
354 progressively significant with an increase of $f\mathbf{Re}_0$ or an increase of the difference between θ and
355 k (e.g., $\theta/k >> 1$ or $\theta/k << 1$). The results and findings of this study may have potential
356 significance and useful implications to the theory and practice of transient pipe flow modelling
357 and analysis such as transient-based pipe faults detection which depends largely on the wave
358 envelope attenuation (amplitude damping) and wave phase change (frequency shift) (Wu and
359 Fricke, 1990; Duan et al., 2012b, 2014; Lee et al., 2013).

360

361 **Experimental Comparison and Results Discussion**

362 In the literature of water supply pipeline systems, there is very few experimental studies for the
363 interaction of transient wave and rough blockages along pipelines. A recent study by the author
364 and his collaborators (Duan et al., 2017) developed a laboratory test system in the hydraulics
365 laboratory at the University of Canterbury in New Zealand to investigate the wave behaviors in a
366 water pipeline with rough blockages. The sketch and principle of the experimental pipeline
367 system and test information is provided in Fig. 5. Particularly, the uniform pipe case (without
368 blockage) is tested for providing reference data for comparative analysis. The rough blockages
369 made of small stone aggregates (glue together with random distribution) were built in the
370 pipeline for testing. Small-amplitude transient waves were generated by the fast closure of side-
371 discharge valve at the downstream end (Fig. 5), and the pressure signals were measured at the
372 immediate upstream of this transient source location for analysis. The transient data were
373 collected by a pressure transducer with a sample frequency of 20 kHz.

374

375 Fig. 5 will be here.

376

377 Based on this laboratory experimental pipeline system designed for Duan et al. (2017),
378 further tests have been conducted for different flow and system conditions (e.g., discharge,
379 roughness and blockages) as listed in Table 1. For convenience, the obtained pressure head traces
380 are normalized by the *Joukowsky* head at downstream valve (denoted as W^* herein) and the time
381 is normalized by the wave time scale along intact pipeline (i.e., $t/(L/a)$, denoted as t^*). The
382 experimental test results for the two cases (intact and blockage) are plotted in Fig. 6. The
383 experimental results of Fig. 6 reveal the significant influence of rough blockage to the transient

384 wave in terms of both amplitude attenuation and phase change. On this point, this result of
385 influence pattern and trend is consistent with the above analytical finding of Eq. (24) in this
386 study.
387
388 Table 1 will be here.
389 Fig. 6 will be here.
390
391 To quantitatively validate the analytical result of Eq. (24), the transient pressure data in Fig.
392 6 are first converted into the frequency domain by the discrete Fourier transform (Lee et al., 2013;
393 Duan et al., 2011a), and then the peak (envelop) data of amplitudes and frequencies are extracted
394 and shown in Figs. 7(a) and 7(b) respectively for further analysis. For comparison, the analytical
395 results by Eq. (24) are also calculated for these two cases and plotted in the same figure.
396
397 Fig. 7 will be here.
398
399 Based on the retrieved data and the test information in Table 1, the overall results of the
400 two factors shown in Fig. 7 demonstrate the good agreement between the analytical solution and
401 experimental data. It can be estimated from these results that the average differences between the
402 analytical and experimental results are within 15% of their mean values for both cases (i.e., about
403 14.1% for amplitude attenuation and 8.7% for frequency shift). By inspection, these differences
404 may be mainly attributed to the following reasons: (1) linearization error of the analytical
405 solution for relatively small amplitude turbulent friction; (2) experimental data error from
406 measurement (sampling frequency and system noises); (3) numerical error occurred in data
407 treatment (discretization and data resolution); and (4) local transient turbulence dissipation

(unsteady friction) in the rough blockage section.

Consequently, the result comparison in Fig. 7 indicates the acceptable accuracy and validity of the derived analytical results in this study for expressing the transient wave scattering phenomenon and process by pipe roughness and blockages in water pipelines. Meanwhile, the results of this study regarding the wave scattering by the rough blockages may provide underlying physics and reasons for the blockage detection errors by the original transient-based methods where only regular blockage configurations have been included (e.g., Stephens, 2008; Duan et al., 2012b; Meniconi et al., 2013, 2015). From this perspective, the analytical results and analysis of this study that have included the roughness and irregularity of pipe-wall and solid blockages may be useful to improve transient modelling and practical applications such as blockage detection in water pipelines (Wu and Fricke, 1990; Brunone et al., 2004; Meniconi et al., 2011; Lee et al., 2013; Duan et al., 2014; Duan et al., 2017; Gong et al., 2014, 2018; Che et al., 2018, 2019; Zouari et al., 2019, 2020; Zanganeh et al., 2020). In this regard, based on the results of current study, the further investigation of transient-based pipe-wall condition assessment (e.g., corrosion, deformation and blockage detection) shall be the next step research work in the future.

Practical Implications and Limitations

The experimental comparison indicates the acceptable accuracy range of the derived analytical solution and results analysis in this study. It is also worthy of noting that the analytical results of this study are derived based on several key assumptions summarized formerly in this paper. In this regard, the potential limitations and practical implications of the results and findings from this study can be summarized as follows.

(1) The analytical results in Eqs. (23) and (24) are in principle valid mainly for relatively small-amplitude transient waves (i.e., $q << Q_0$). According to Meniconi et al. (2011), however, such small-amplitude transient events (either naturally happened or artificially generated) are commonly existent in urban water supply systems and utilized for water pipeline diagnosis;

(2) The analysis results in Figs. 3 and 4 are based on typical configuration parameters in urban water supply pipelines. Nevertheless, the analytical results can also be easily extended to other fluid piping systems, as long as the transient flow model is still valid (or approximately valid) for such systems. For instance, the incorporation of viscoelastic term (pipe-wall deformation) in the continuity equation (1), coupling with the results of rough blockages in this study, will be useful to the arterial blood system analysis (Mei and Jing, 2016);

(3) In this study, an experimental test system was designed in the laboratory, in which the artificially fabricated rough blockages were used in the tests. Despite these tests might not be able to represent exactly the practical situations in water supply pipelines, the obtained results herein may provide a lumped effect of transient wave scattering and dynamic response as propagating in a pipeline with rough blockages (e.g., amplitude damping and phase shifting).

For higher order (i.e., order > 2) perturbations induced during transient wave propagation process in water pipelines, such as high frequency wave behavior (e.g., $\omega \sim a/D$), advanced analytical methodology, probably together with high-dimensional (2D/3D) numerical simulation techniques (Louati and Ghidaoui, 2019), will be required to derive the solutions to the nonlinear transient wave interactions. Based on the results and findings of this study, the further investigation of high-order wave behavior is expected to be useful to enhance the pipeline condition assessment under complex system conditions (such as transient-based leak and blockage detection).

454

455 **Summary and Conclusions**

456 This paper investigates transient wave propagation behaviors under the conditions of rough
457 blockages (causing irregular pipe diameter variations) and pipe-wall roughness. An analytical
458 result is derived in the study by multi-scale wave perturbation analysis method for describing the
459 wave scattering effect due to both factors of pipe blockages and pipe-wall roughness along the
460 pipeline under the condition of transient laminar and small-amplitude turbulent flows. The
461 relevance and importance of these two factors are discussed for their effects on transient wave
462 modifications (envelope attenuation and phase change).

463 The obtained analytical results indicate that the relative importance of pipe blockage and
464 pipe-wall roughness to wave behaviors can be expressed by two dimensionless factors G_{amp} and
465 G_{pha} defined in Eq. (27) in this study. Specifically, these two factors are functions of incidence
466 wave properties (wave length and speed) and pipeline conditions (roughness, blockage range and
467 severity). The dominant influence domains of these two effects are analyzed and discussed for
468 typical ranges of pipe parameters and flow conditions in water pipeline systems. The result
469 shows that the pipe-wall roughness effect on wave modification becomes significant only when
470 $f\mathbf{Re}_0 > 10^2$ and ($\theta/k > 10$ or $\theta/k < 10$) for the demonstration case, otherwise the rough blockage
471 induced wave scattering effect will be dominant to the wave behavior.

472 These key findings from the analytical analysis have been compared and validated by
473 experimental data from laboratory tests, indicating that the results of this study may provide
474 useful implications on the transient wave modelling and utilization for pipeline diagnosis (e.g.,
475 leak and blockage detection) in the water pipeline system. In particular, the inclusion of the wave
476 scattering effect by rough blockages will be beneficial to improve the accuracy and applicability

of the transient-based defect detection method, which is commonly developed for small-amplitude wave operations and tested for laminar (or low turbulent) flow conditions (e.g., Meniconi et al., 2011). Furthermore, with the two dimensionless factors derived in this study, the transient data measured from practical pipeline systems may be better interpreted by considering the wave scattering effect from different reasons (internal blockage, pipe-wall roughness, etc.). It is also noted that more applications under different complex systems and operation conditions are required in future work to further validate and verify the results and findings of this study.

Data Availability Statement

Some or all data, models, or code generated or used during the study are available from the corresponding author by request (including analytical derivation, numerical model data and experimental test data).

Acknowledgement

This research was supported by the Hong Kong Research Grants Council (RGC) (15201017, 15200719) and the National Natural Science Foundation of China (51639007).

Notation

The following symbols are used in this paper:

A	=	pipe cross-sectional area
a	=	wave speed
A_0	=	pipe cross-sectional area for uniform pipeline
D	=	pipe diameter

500	f	=	Darcy friction factor
501	K	=	friction coefficient
502	$K\omega$	=	friction effects to the mainstream wave propagation
503	k	=	wave number
504	M	=	March number
505	P	=	pressure
506	P_0	=	initial steady-state pressure
507	p	=	transient parts of pressure
508	Q	=	flowrate
509	Q_0	=	initial steady-state flowrate
510	q	=	transient parts of flowrate
511	Re	=	initial Reynolds number
512	T_d	=	radial wave diffusion time scale
513	T_w	=	longitudinal wave propagation time scale
514	t	=	temporal coordinate
515	v	=	kinematic viscosity
516	W	=	wave amplitude
517	X	=	characteristic distance for wave propagation
518	x	=	spatial coordinate
519	Y	=	characteristic phase for wave propagation
520	α	=	friction-related dimensionless damping factor
521	δ	=	spatial distance
522	ε	=	scaling variable

523 ϕ = dimensionless factor representing for wave phase change

524 $\gamma(\delta)$ = correlation coefficient

525 σ^2 = ensemble averaged magnitude of pipe area disorders

526 θ = spatial correlation factor of pipe disorders

527 τ_w = wall shear stress

528 τ_{w0} = average (steady) components of wall shear stress

529 τ_w^p = perturbing (transient) components of wall shear stress

530 ω = wave frequency

531 ψ = dimensionless factor representing for wave envelope attenuation

532 $\zeta(x)$ = irregular variation of pipe cross-sectional area

533

534 **References**

535 Ayati, A., Haghighi, A., and Lee, P.J. (2019). Statistical Review of Major Standpoints in
536 Hydraulic Transient-Based Leak Detection. Journal of Hydraulic Structures, 5(1), 1-26.

537 Bergant, A., Simpson, A.R., and Tijsseling, A.S. (2006). Water hammer with column separation:
538 A historical review. Journal of Fluids and Structures, 22(2), 135-171.

539 Brunone, B. (1999). Transient test-based technique for leak detection in outfall pipes. Journal of
540 Water Resources Planning and Management, ASCE, 125(5), 302-306.

541 Brunone, B., Ferrante, M., and Cacciamani, M. (2004). Decay of pressure and energy dissipation
542 in laminar transient flow. Journal of Fluids Engineering, ASME, 126(6), 928-934.

543 Brunone, B., and Berni, A. (2010). Wall shear stress in transient turbulent pipe flow by local
544 velocity measurement, Journal of Hydraulic Engineering, ASCE, 136(10), 716-726.

545 Chaudhry M.H. (2014). Applied Hydraulic Transients (3rd Edition). Springer, New York.

546 Che, T.C., Duan, H.F., Lee, P.J., Pan, B., and Ghidaoui, M.S. (2018). Transient frequency
547 responses for pressurized water pipelines containing blockages with linearly varying
548 diameters. Journal of Hydraulic Engineering, ASCE, 144(8), 04018054.
549 Che, T.C., Duan, H.F., Pan, B., Lee, P.J., and Ghidaoui, M.S. (2019). Energy analysis of the
550 resonant frequency shift pattern induced by non-uniform blockages in pressurized water
551 pipes. Journal of Hydraulic Engineering, ASCE, 145(7), 04019027.
552 Colton, D., Coyle, J., and Mon, P. (2000). Recent developments in inverse acoustic scattering
553 theory. SIAM Review, 42(3), 369-414.
554 Covas, D., Stoianov, I., Mano, J.F., Ramos, H., Graham, N., and Maksimovic, C. (2005). The
555 dynamic effect of pipe-wall viscoelasticity in hydraulic transients. Part II–model
556 development, calibration and verification. Journal of Hydraulic Research, IAHR, 43(1), 56-
557 70.
558 Duan, H.F., Tung, Y.K., and Ghidaoui, M.S. (2010a). Probabilistic analysis of transient design
559 for water supply systems. Journal of Water Resources Planning and Management,
560 ASCE,136(6), 678-687.
561 Duan, H.F., Ghidaoui, M.S., Lee, P.J., Tung, Y.K. (2010b). Unsteady friction and visco-elasticity
562 in pipe fluid transients. Journal of Hydraulic Research, IAHR, 48(3), 354-362.
563 Duan, H.F., Lee, P.J., Ghidaoui, M.S., and Tung, Y.K. (2011a). Leak detection in complex series
564 pipelines by using system frequency response method. Journal of Hydraulic
565 Research, IAHR, 49(2), 213–221.
566 Duan, H.F., Lu, J.L., Kolyshkin, A.A., and Ghidaoui, M.S. (2011b). The effect of random
567 inhomogeneities on wave propagation in pipes. Proceedings of the 34th IAHR Congress,
568 June 26 – July 1, 2011, ISBN 978-0-85825-868-6, Engineers Australia, Australia.

569 Duan, H.F., Ghidaoui, M.S., Lee, P.J., and Tung, Y.K. (2012a). Relevance of unsteady friction to
570 pipe size and length in pipe fluid transients. Journal of Hydraulic Engineering, ASCE,
571 138(2), 154-166.
572 Duan, H.F., Lee, P.J., Ghidaoui, M.S., and Tung, Y.K. (2012b). Extended blockage detection in
573 pipelines by using the system frequency response analysis. Journal of Water Resources
574 Planning and Management, ASCE, 138(1), 55-62.
575 Duan, H.F., Lee, P.J., Ghidaoui, M.S., and Tuck, J. (2014). Transient wave-blockage interaction
576 and extended blockage detection in elastic water pipelines. Journal of Fluids and Structures,
577 46, 2-16.
578 Duan, H.F., and Lee, P.J. (2016). Transient-based frequency domain method for dead-end side
579 branch detection in reservoir pipeline-valve systems. Journal of Hydraulic Engineering,
580 ASCE, 142(2), 04015042.
581 Duan, H.F. (2017). Transient wave scattering and its influence on transient analysis and leak
582 detection in urban water supply systems: theoretical analysis and numerical
583 validation. Water, MDPI, 9(10), 789.
584 Duan, H.F., Lee, P.J., Che, T.C., Ghidaoui, M.S., Karney, B.W., and Kolyshkin, A.A. (2017).
585 The influence of non-uniform blockages on transient wave behavior and blockage detection
586 in pressurized water pipelines. Journal of Hydro-environment Research, 17, 1-7.
587 Duan, H.F., Che, T.C., Lee, P.J., and Ghidaoui, M.S. (2018). Influence of nonlinear turbulent
588 friction on the system frequency response in transient pipe flow modelling and
589 analysis. Journal of Hydraulic Research, IAHR, 56(4), 451-463.
590 Ebacher, G., Besner, M., Lavoie, J., Jung, B., Karney, B., and Prévost, M. (2011). Transient
591 modeling of a full-scale distribution system: comparison with field data. Journal of Water

592 Resources Planning and Management, ASCE, 137(2), 173-182.
593 Ghidaoui, M.S., Zhao, M., McInnis, D.A., and Axworthy, D.H. (2005). A review of water
594 hammer theory and practice. Applied Mechanics Reviews, ASME, 58(1), 49-76.
595 Gong J., Lambert M.F., Simpson A.R., and Zecchin A.C. (2014). Detection of localized
596 deterioration distributed along single pipelines by reconstructive MOC analysis. Journal of
597 Hydraulic Engineering, ASCE, 140(2), 190-198.
598 Gong J., Lambert, M.F., Zecchin A.C., and Simpson A.R. (2016). Experimental verification of
599 pipeline frequency response extraction and leak detection using the inverse repeat
600 signal. Journal of Hydraulic Research, IAHR, 54(2), 210-219.
601 Gong J., Lambert M.F., Nguyen S., Zecchin A.C., and Simpson, A.R. (2018). Detecting thinner-
602 walled pipe sections using a spark transient pressure wave generator. Journal of Hydraulic
603 Engineering, ASCE, 144(2), 06017027.
604 Guidara, M.A., Taieb, L.H., Schmitt, C., Taieb, E.H., and Azarib, Z. (2018). Investigation of
605 viscoelastic effects on transient flow in a relatively long PE100 pipe. Journal of Fluids and
606 Structures, 80, 370-389.
607 Keramat, A., Tijsseling, A.S., Hou, Q., Ahmadi, A. (2012). Fluid-structure interaction with pipe-
608 wall viscoelasticity during water hammer. Journal of Fluids and Structures, 28, 434-455.
609 Keramat, A., Ghidaoui, M.S., Wang, X., and Louati, M. (2020). Cramer-Rao lower bound for
610 performance analysis of leak detection. Journal of Hydraulic Engineering, ASCE, 145(6),
611 04019018.
612 Kim, S.H. (2016). Impedance method for abnormality detection of a branched pipeline system.
613 Water Resources Management, 30(3), 1101-1115.
614 Kim, S.H. (2020). Multiple leak detection algorithm for pipe network. Mecahnical Systems and

615 Signal Procesing, 139, 106645.
616 Lee, P.J., Duan, H.F., Ghidaoui, M.S., and Karney, B.W. (2013). Frequency domain analysis of
617 pipe fluid transient behaviors. Journal of Hydraulic Research, IAHR, 51(6), 609-622.
618 Lee, P.J., Duan, H.F., Tuck, J., and Ghidaoui, M.S. (2015). Numerical and experimental
619 illustration of the effect of signal bandwidth on pipe condition assessment using fluid
620 transients. Journal of Hydraulic Engineering, ASCE, 141(2), 014074.
621 Louati, M., and Ghidaoui, M.S. (2019). The need for high order numerical scheme for modeling
622 dispersive high frequency acoustic waves in water-filled pipe. *Journal of Hydraulic*
623 *Research,* IAHR, 57(3), 405-425.
624 Lu, Z. (2008). Stochastic modelling of unsteady open channel flow and reliability analysis. PhD
625 Dissertation, Department of Civil and Environmental Engineering, The Hong Kong
626 University of Science and Technology, Hong Kong.
627 McInnis D. and Karney B.W. (1995). Transients in distribution networks: field tests and demand
628 models. Journal of Hydraulic Engineering, ASCE, 121(3), 218-231.
629 Mei, C.C. and Jing, H.X. (2016). Pressure and wall shear stress in blood hammer – analytical
630 theory. Mathematical Biosciences, 280, 62-70.
631 Meniconi, S., Brunone, B., Ferrante, M., and Massari, C. (2011). Small amplitude sharp pressure
632 waves to diagnose pipe systems. Water Resources Management, 25(1), 79-96.
633 Meniconi, S., Brunone, B., and Ferrante, M. (2012). Water-hammer pressure waves interaction at
634 cross-section changes in series in viscoelastic pipes. Journal of Fluids and Structures, 33,
635 44-58.
636 Meniconi, S., Duan, H.F., Lee, P.J., Brunone, B., Ghidaoui, M.S., and Ferrante, M. (2013).
637 Experimental investigation of coupled frequency- and time-domain transient test-based

638 techniques for partial blockage detection in pipelines. Journal of Hydraulic Engineering,
639 ASCE, 139(10), 1033-1040.
640 Meniconi S., Brunone B., Ferrante M., Capponi C., Carrettini C.A., Chiesa C., Segalini D., and
641 Lanfranchi E.A. (2015). Anomaly pre-localization in distribution–transmission mains by
642 pump trip: preliminary field tests in the Milan pipe system. Journal of Hydroinformatics,
643 IWA, 17(3), 377-388.
644 Pan, B., Duan, H.F., Meniconi, S., Urbanowicz, K., Che, T.C., and Brunone, B.
645 (2020). Multistage frequency-domain transient-based method for the analysis of viscoelastic
646 parameters of plastic pipes. Journal of Hydraulic Engineering, ASCE, 146(3), 04019068.
647 Pan, B., Duan, H.F., Meniconi, S., and Brunone, B. (2021). FRF-based transient wave analysis
648 for the viscoelastic parameters identification and leak detection in water-filled plastic
649 pipes. Mechanical Systems and Signal Processing (MSSP), 146, 107056.
650 Ramezani, L., and Karney, B. (2017). Water column separation and cavity collapse for pipelines
651 protected with air vacuum valves: understanding the essential wave processes. Journal of
652 Hydraulic Engineering, ASCE, 143(2), 04016083.
653 Stephens, M.L. (2008). Transient response analysis for fault detection and pipeline wall
654 condition assessment in field water transmission and distribution pipelines and networks.
655 PhD Thesis, School of Civil, Environmental and Mining Engineering, The University of
656 Adelaide, South Australia.
657 Vardy, A.E., and Brown, J.M. (1995). Transient, turbulent, smooth pipe friction, Journal of
658 Hydraulic Research, IAHR, 33(4), 435-456.
659 Wang, X., and Ghidaoui M.S. (2018). Pipeline leak detection using the matched-field processing
660 method. Journal of Hydraulic Engineering, ASCE, 144(6), 04018030.

661 Wang, X., Palomar, D.P., Zhao, L.C., and Ghidaoui M.S. (2019). Spectral-based methods for
662 pipeline leakage localization. Journal of Hydraulic Engineering, ASCE, 145(3), 04018089.
663 Wiggert, D.C., and Tijsseling, A.S. (2001). Fluid transients and fluid-structure interaction in
664 flexible liquid-filled piping. Applied Mechanics Reviews, ASME, 54(5), 455-481.
665 Wright, S., Lewis, J., and Vasconcelos, J. (2011). Geysering in rapidly filling storm-water
666 tunnels. Journal of Hydraulic Engineering, ASCE, 137(1), 112-115.
667 Wu, Q., and Fricke, F. (1990). Determination of blocking locations and cross-sectional area in a
668 duct by eigenfrequency shifts. Journal of the Acoustical Society of America, 87(1), 67-75.
669 Wylie, E.B., Streeter, V.L., and Suo, L. (1993). Fluid Transient in Systems, Prentice-Hall,
670 Englewood Cliffs.
671 Zanganeh, R., Jabbari, E., and Tijsseling, A., and Keramat, A. (2020). Fluid-structure interaction
672 in transient-based extended defect detection of pipe walls. Journal of Hydraulic Engineering,
673 ASCE, 146(4), 04020015.
674 Zhou, L., Liu, D., and Karney, B. (2013). Investigation of hydraulic transients of two entrapped
675 air pockets in a water pipeline. Journal of Hydraulic Engineering, ASCE, 139(9), 949-959.
676 Zhu, Y., Duan, H.F., Li, F., Wu, C.G., Yuan, Y.X., and Shi, Z.F. (2018). Experimental and
677 numerical study on transient air-water mixing flows in viscoelastic pipes. Journal of
678 Hydraulic Research, IAHR, 56(6), 877-887.
679 Zouari, F., Blåsten, E., Louati, M, and Ghidaoui, M.S. (2019). Internal pipe area reconstruction
680 as a tool for blockage detection. Journal of Hydraulic Engineering, ASCE, 145(6),
681 04019019.
682 Zouari, F., Louati, M, Meniconi, S., Blåsten, E., Ghidaoui, M.S., and Brunone, B. (2020).
683 Experimental verification of the accuracy and robustness of area reconstruction method for

684 pressurized water pipe System. Journal of Hydraulic Engineering, ASCE, 146(3), 04020004.

Table 1. Settings for experimental test systems.

Test case	Uniform pipe sections				Blockage section (average)				**Re_0** ($\times 10^3$)
	L_1 (m)	L_3 (m)	D_1 (=D_3) (mm)	a_1 (=a_3) (m/s)	L_b (m)	D_b (mm)	a_b (m/s)	σ^2	
Blockage-free (intact)	15.5	20.4	73.2	1180	5.6	73.2	1180	0	2.0 ~ 15.0
Rough blockage (aggregate)	15.5	20.4	73.2		5.6	59.3	1050	0.01	

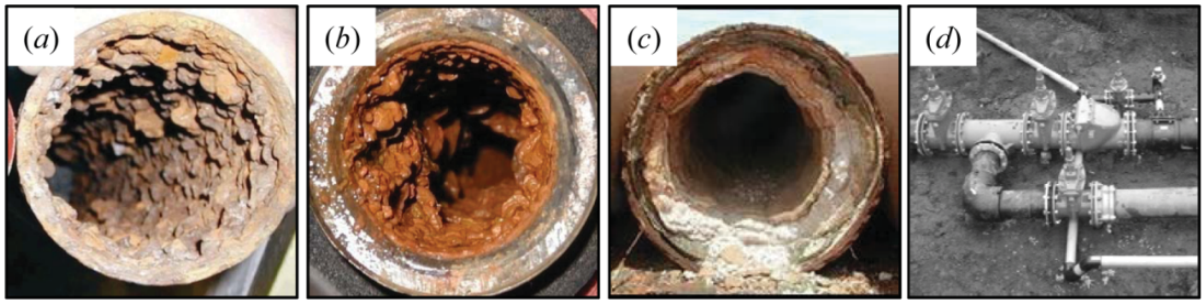

Fig. 1. Disorders of pipe diameters (roughness and blockages) in water pipelines due to different factors: (a) corrosion; (b) bio-film; (c) deposition; (d) complex connection.

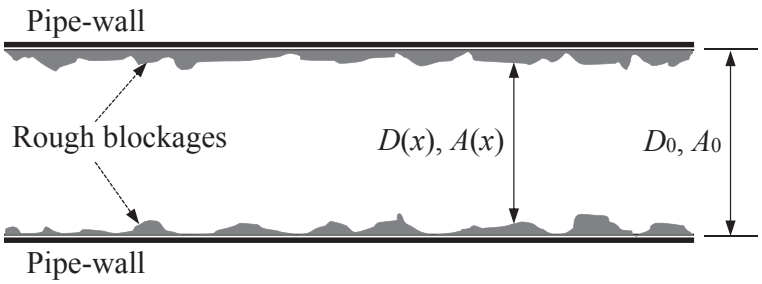

Fig. 2. Sketch of rough blockage configuration in a water pipe section.

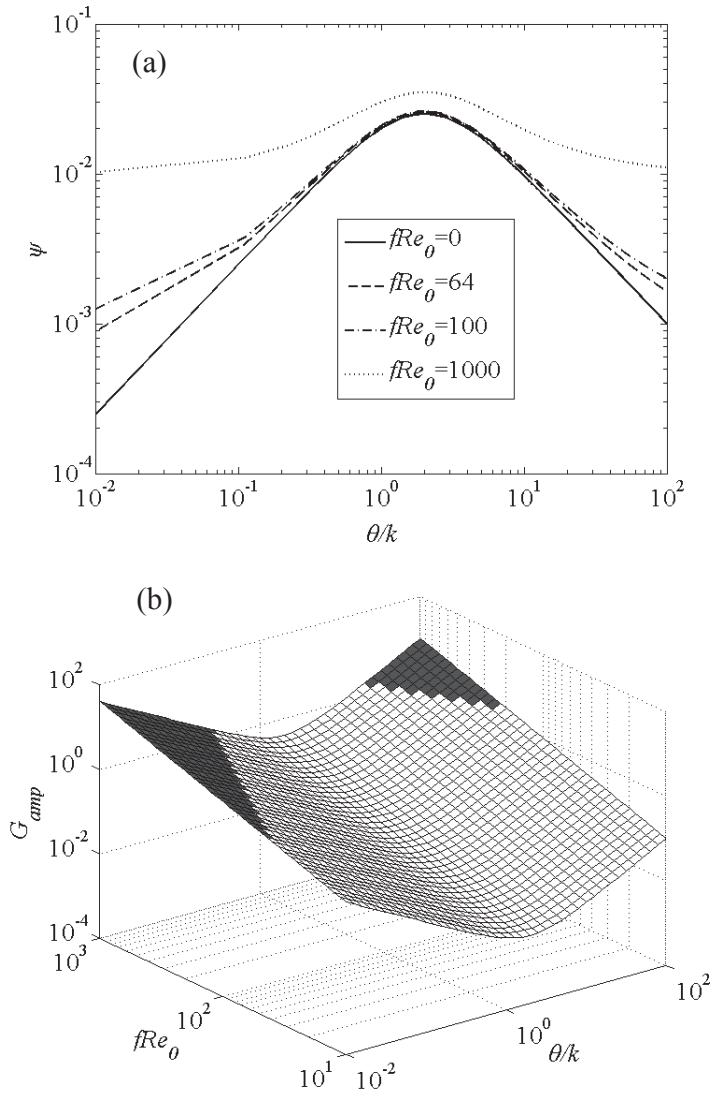

Fig. 3. Effects of pipe wall roughness and blockage on transient wave envelope attention: (a): dimensionless envelope attenuation coefficient (ψ); (b): relative importance (G_{amp}) with the black-filled region for $G_{amp} > 1$.

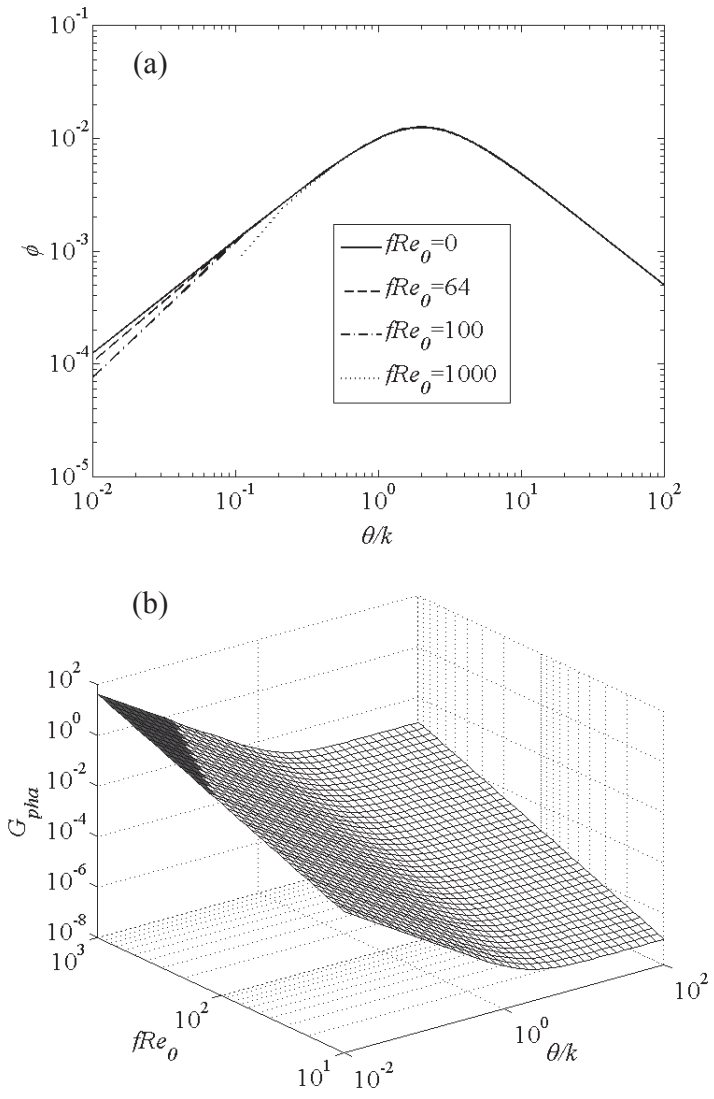

Fig. 4. Effects of pipe wall roughness and blockage on transient wave phase change: (a): dimensionless phase change coefficient (ϕ); (b): relative importance (G_{pha}) with the black-filled region for $G_{pha} > 1$.

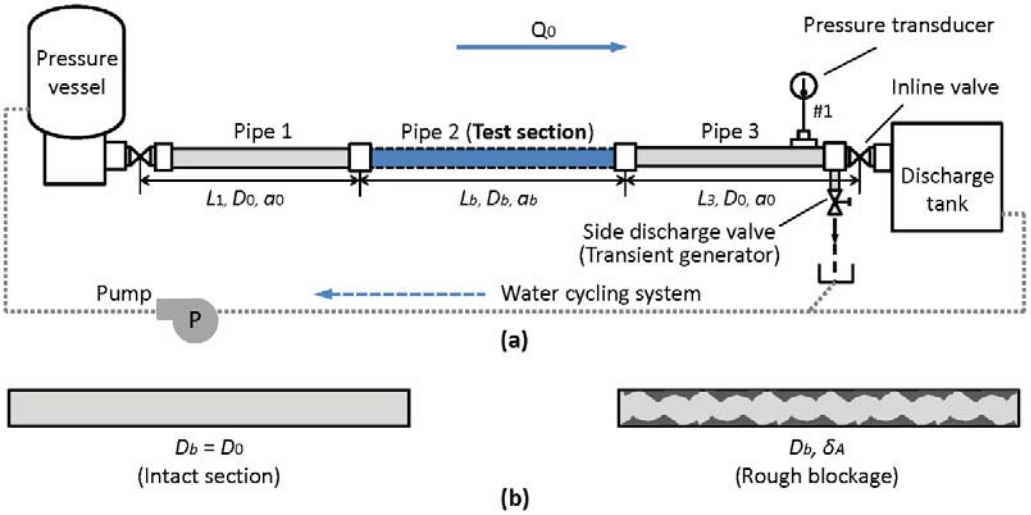

Fig. 5. Experimental test system: (a) sketch of test system configuration; (b) inserted sections for the two test cases (intact and rough blockage sections).

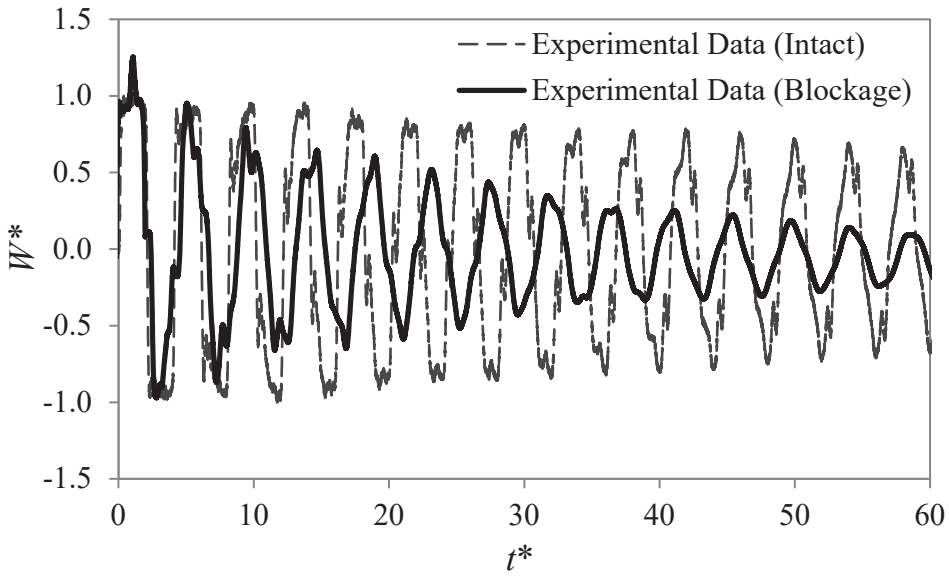

Fig. 6. Time-domain measurement of transient waves for two test cases (0~60 L/a).

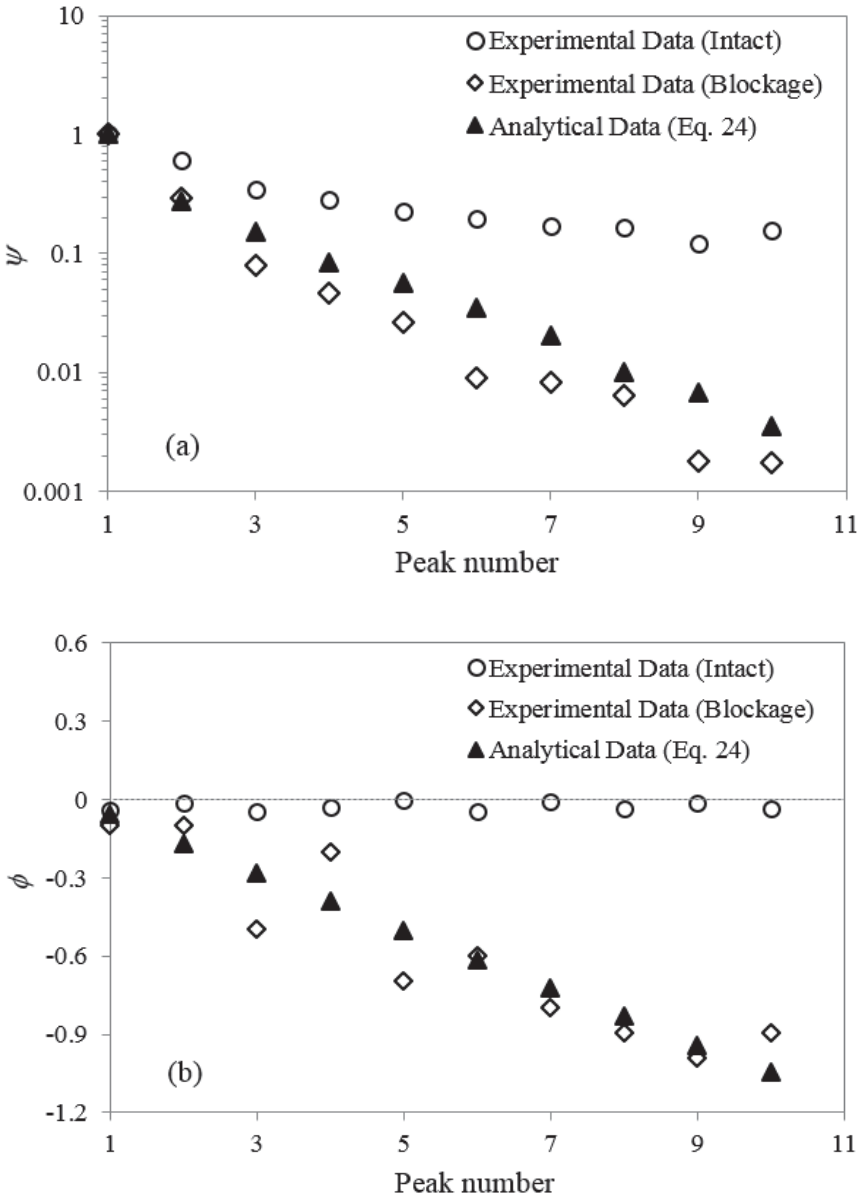

Fig. 7. Frequency-domain results of two test cases (with first 10 peaks) for: (a): peak amplitude attenuation; (b): peak frequency shift (phase change).

List of Figure Captions

Fig. 1. Disorders of pipe diameters (roughness and blockages) in water pipelines due to different factors: (a) corrosion; (b) biofilm; (c) deposition; (d) complex connection

Fig. 2. Sketch of rough blockage configuration in a water pipe section

Fig. 3. Effects of pipe wall roughness and blockage on transient wave envelope attention: (a): dimensionless envelope attenuation coefficient (ψ); (b): relative importance (G_{amp}) with the black-filled region for $G_{amp} > 1$

Fig. 4. Effects of pipe wall roughness and blockage on transient wave phase change: (a): dimensionless phase change coefficient (ϕ); (b): relative importance (G_{pha}) with the black-filled region for $G_{pha} > 1$

Fig. 5. Experimental test system: (a) sketch of test system configuration; (b) inserted sections for the two test cases (intact and rough blockage sections)

Fig. 6. Time-domain measurement of transient waves for two test cases (0~60 L/a)

Fig. 7. Frequency-domain results of two test cases (with first 10 peaks) for: (a): peak amplitude attenuation; (b): peak frequency shift (phase change)